J Electr Eng Technol.2015; 10(3): 971-982
http://dx.doi.org/10.5370/JEET.2015.10.3.971

ISSN(Print) 1975-0102
ISSN(Online) 2093-7423

The Power Analysis and Its Control of Two-phase Orthogonal Power Supply for the Continuous Casting

Fujun Ma†, An Luo* and Qiaopo Xiong**

Abstract – In order to improve the quality of the billet continuous casting, a two-phase orthogonal power supply (TPOPS) for electromagnetic stirrer is researched, which is composed of three-phase PWM rectifier and three-leg inverter. According to the power analysis of system, the ripple of dc-link voltage is analyzed and its analytical expression is derived. In order to improve the performance of electromagnetic stirring, an integrated control method with feedforward control is proposed for PWM rectifier to suppress the fluctuations of dc-link voltage and provide a stable dc source for inverter. According to the simplified equivalent model, a composite current control method is proposed for inverter. This proposed method can combine the merits of feedforward control with feedback control to effectively improve the dynamic output performance of TPOPS. Finally, a 300kVA prototype of TPOPS is developed, and the results have verified the analysis and control method.

Keywords: Electromagnetic stirrer, Three-leg inverter, PWM rectifier, Power balance, Feedforward control, Feedback control

1. Introduction

Special steel is the key material of major equipment manufacturers, construction projects and defense advanced weapons, and the quality of special steel has a very important influence on the manufacturing level. Currently, the electromagnetic (EM) stirring technology is a key technical way to improve the quality of special billet [1, 2]. By using different forms of magnetic generators to produce a moved magnetic field, a powerful EM stirring force can be induced in the molten steel. The EM stirring force can be used to control the flow and solidification of the molten steel in the continuous casting process, and then it can expand the equiaxed crystal zone and reduce the center porosity to improve the quality of steel products [3, 4].

Nowadays, the structure of two-phase orthogonal power supply (TPOPS) is widely used in the continuous casting process. TPOPS can output two-phase orthogonal currents to power two coils, and then form a rotating EM stirring force to excite a rotary motion of molten steel [5, 6]. In terms of the topology of TPOPS, it is always composed of three-phase rectifier and two-phase inverter. The former rectifier of TPOPS generally adopts three-phase uncontrolled rectifier [7, 8], thus the content of harmonic currents is high. According to the requirements of continuous casting, alternate rotation is needed to make the EM stirring of molten steel more uniformly. As the output currents of TPOPS will change rapidly in the alternate process, the energy of induction coils will vary dramatically. The energy of dc-link capacitor cannot be quickly released and absorbed by the uncontrolled rectifier, which can lead to significant fluctuations of dc-link voltage and affect the normal control of back inverter. As for the topology of two-phase inverter, four legs were adopted to form two single-phase full-bridge inverters [9], so they can be controlled separately. This structure has high utilization rate of dc-link voltage, but the number of power switches is 8. Therefore, two legs were proposed to form a two-phase inverter in [10], which can be considered as two single-phase half-bridge inverters and they were shared with dc-link capacitors. This structure only needs 4 power switches, however, the utilization rate of dc-link voltage is low and a voltage-balanced control is needed for two dc-link capacitors. Therefore, in order to make up for their defects, a two-phase three-leg inverter (TPTLI) was put forward in [11, 12], in which two legs were independent and the third leg was for public use. According to the analysis above, a TPTLI is adopted for TPOPS in the paper. Meanwhile, in order to improve power quality of system and maintain a stable dc voltage for inverter, a three-phase pulse width modulation (PWM) rectifier is adopted.

As for the control of TPOPS, the references were mainly discussed about the control methods of back inverter. In [11], a set of output filters was adopted by TPTLI for EM stirrer, and a deadbeat control method of TPTLI based on the switching model was derived. In [13-15], a proportional-integral (PI) control or hysteresis control was used by two-phase inverter to achieve current closed-loop control, and then the control system adopted sinusoidal PWM method to generate switching signals to drive power

† Corresponding Author: College of Electrical and Information Engineering, Hunan University, China. (mafujun2004@163.com)
* College of Electrical and Information Engineering, Hunan University, China. (an_luo@126.com)
** 722th Research Institute of CSIC, Wuhan, Hubei Province, China. (403864117@qq.com)
Received: June 22, 2014; Accepted: November 18, 2014

switches. In [16], a synchronous frame current control scheme was proposed for voltage-source inverter to drive a two-phase linear motor. Later, space-vector modulation (SVM) methods were proposed for TPTLI to improve the utilization rate of dc-link voltage [12, 17, 18], which can enhance the output capacity of TPTLI for two-phase motors. However, fast positive and negative alternate rotations are needed to make the EM stirring of molten steel more symmetrically and uniformly, so the output currents of TPOPS have to be changed rapidly in the casting process. According to this requirement, TPOPS is expected to have a fast dynamic tracking performance, while the control method of TPOPS is the key section to meet the satisfactory stirring performance.

In order to improve the performance of power supply, the control method of TPOPS is researched in the paper. Firstly the power model of system is analyzed, and the ripple of dc-link voltage is derived mathematically according to the power analysis in Scetion.II. Then an integrated control method with feedforward control for PWM rectifier is proposed in Scetion.III, and a ripple elimination method for voltage control is presented. According to the simplified equivalent circuit of EM stirrer, a composite current control method is proposed for TPTLI in Scetion.VI, and its closed-loop tracking performance is analyzed. Finally, the prototype of TPOPS is developed, meanwhile, the simulation and experimental results have been carried out to verify the analysis and control method.

2. The Topology of TPOPS and its Power Analysis

The topology of TPOPS for EM stirrer in the billet continuous casting is shown as Fig. 1. It is composed of a PWM rectifier and a TPTLI. The PWM rectifier is adopted to eliminate the harmonic currents, improve the power factor (PF) of TPOPS, and maintain dc-link voltage stably. The PWM rectifier is connected with the three-phase grid by filter inductor L_o. The load EM stirrer is two-phase induction coils installed in the cooling water. In order to filter higher harmonics and prevent over-current when short-circuit fault happens, a set of output filter L is adopted. The operation principle of TPOPS is shown as follows: firstly, the three-phase ac voltage sources are converted into a dc voltage source by PWM rectifier, and then it can be converted into two-phase ac sources to supply EM stirrer by TPTLI. The operation principle of EM stirrer is similar to the two-phase asynchronous induction motor [19, 20]. Shown as Fig. 1, the load two-phase induction coils, which can be considered as the stator, are installed around the crystallizer of molten steel. And the induction coils can generate a rotating magnetic field and motion in the molten steel which is considered as the rotor. The features of rotary motion are directly related with the amplitude and frequency of output currents of TPTLI. According to the attribute requirements of different kinds of steel, the expected output currents of TPTLI are different.

2.1 The input power calculation of TPOPS

In order to study the operation of TPOPS, the output and input power of system is analyzed. Assuming the three-phase voltages of power grid are:

$$\begin{cases} u_{sa} = U\sin\omega_o t \\ u_{sb} = U\sin(\omega_o t - 2\pi/3) \\ u_{sc} = U\sin(\omega_o t + 2\pi/3) \end{cases} \tag{1}$$

Where, U is the amplitude of phase voltage, ω_o is the angular frequency of power grid. PWM rectifier can achieve a unit PF rectification by the closed-loop control. Assuming three-phase input currents of PWM rectifier are:

$$\begin{cases} i_{ca} = I_p\sin\omega_o t \\ i_{cb} = I_p\sin(\omega_o t - 2\pi/3) \\ i_{cc} = I_p\sin(\omega_o t + 2\pi/3) \end{cases} \tag{2}$$

Where, I_p is the amplitude of active current. Assuming the active power of load EM stirrer is P_d. If ignore the power loss of TPOPS, then there is:

$$I_p = 2P_d / 3U \tag{3}$$

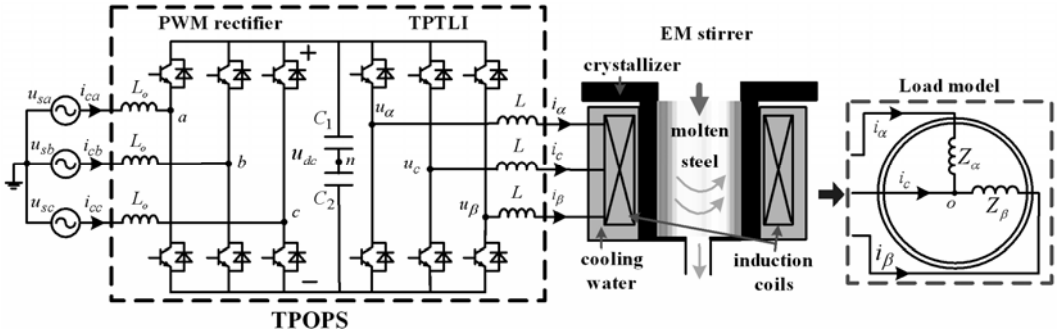

Fig. 1. The topology of TPOPS for EM stirring

As the inductance of input filter inductor is L_o, and its resistance is small and ignored here. The three-phase voltages of filter inductors can be obtained as:

$$\begin{cases} u_{La} = L_o di_{ca} / dt = \omega_o L_o I_p \sin(\omega_o t + \pi/2) \\ u_{Lb} = L_o di_{cb} / dt = \omega_o L_o I_p \sin(\omega_o t - \pi/6) \\ u_{Lc} = L_o di_{cc} / dt = \omega_o L_o I_p \sin(\omega_o t + 7\pi/6) \end{cases} \quad (4)$$

The total input power of PWM rectifier is:

$$\begin{aligned} P_{in} &= P_S - P_L \\ &= u_{sa} i_{ca} + u_{sb} i_{cb} + u_{sc} i_{cc} - u_{La} i_{ca} - u_{Lb} i_{cb} - u_{Lc} i_{cc} \\ &= 3UI_p / 2 \end{aligned} \quad (5)$$

Where, P_S is the power generated by three-phase gird, and it is $3UI_p/2$; P_L is the power generated by three-phase filter inductors, and it is 0.

2.2 The output power calculation of TPOPS

The load of TPOPS is the EM stirrer shown as Fig. 1. The operation principle of EM stirrer is similar to asynchronous induction motor. Two-phase induction coils are considered as the stator of motor, while the rotating molten steel can be considered as the rotor. According to the equivalent model of asynchronous induction motor in [19, 20], the equivalent circuit of EM stirrer can be established shown as Fig. 2. Assuming $L_{\delta 1}$, $r_{\delta 1}$ are the equivalent leakage inductance and resistance of induction coils respectively; $L_{\delta 2}$, $r_{\delta 2}$ are the equivalent inductance and resistance of EM stirrer's rotor respectively.

At the rated operation status, the excitation reactance X_N meets: $|X_N| > 10 * |r_{\delta 2} / S_n + j\omega L_{\delta 2}|$ (ω is output angular frequency; S_n is the slip ratio). Therefore, the excitation reactance can be neglected. Meanwhile, the flow speed of molten steel is slow and the slip ratio S_n is always high according to the engineering practice. In order to facilitate analysis, assuming the slip ratio is equal to 1, so the equivalent resistance $r_{\delta 2} / S_n$ can be simplified as $r_{\delta 2}$. The simplified equivalent circuit of EM stirrer can be shown as Fig. 2(b). According to the rated parameters, the equivalent parameters of EM stirrer can be obtained as follows:

$$\begin{cases} r_{\delta 1} + r_{\delta 2} = P_M / (2I_N^2) \\ L_{\delta 1} + L_{\delta 2} = Q_M / (2I_N^2) / \omega \end{cases} \quad (6)$$

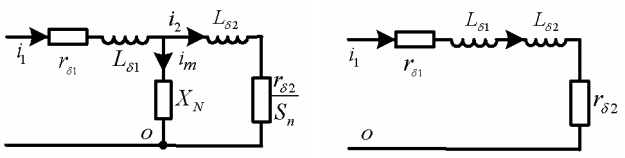

(a) the equivalent circuit (b) the simplified equivalent circuit

Fig. 2. The equivalent circuit of EM stirrer

Where, P_M and Q_M are the rated output active and reactive power of EM stirrer respectively; I_N is the rated output current. The α - and β -phase equivalent impedance for three-leg inverter can be obtained as:

$$\begin{cases} Z_\alpha = r_1 + j\omega L_1 = (r_{\delta 1} + r_{\delta 2}) + j\omega(L_{\delta 1} + L_{\delta 2}) \\ Z_\beta = r_2 + j\omega L_2 = (r_{\delta 1} + r_{\delta 2}) + j\omega(L_{\delta 1} + L_{\delta 2}) \end{cases} \quad (7)$$

where, there are $r_1 = r_2 = r_{\delta 1} + r_{\delta 2}$ and $L_1 = L_2 = L_{\delta 1} + L_{\delta 2}$. According to Fig. 1 and (7), the output voltages of three-leg inverter can be equivalent as:

$$\begin{cases} u_{\alpha o} = Ldi_\alpha / dt + ri_\alpha + L_1 di_\alpha / dt + r_1 i_\alpha \\ u_{\beta o} = Ldi_\beta / dt + ri_\beta + L_2 di_\beta / dt + r_2 i_\beta \\ u_{co} = Ldi_c / dt + ri_c \end{cases} \quad (8)$$

where, L, r are the inductance and resistance of output filters respectively shown as Fig. 1. Assuming $i_\alpha = I_m \sin \omega t$, $i_\beta = I_m \cos \omega t$, and then there is:

$$i_c = -(i_\alpha + i_\beta) = -\sqrt{2} I_m \sin(\omega t + \pi/4) \quad (9)$$

where, I_m is the amplitude of output currents, ω is output angular frequency of inverter. Then the output voltages can be expressed as:

$$\begin{cases} u_{\alpha o} = \omega L_m I_m \sin(\omega t + \pi/2) + r_m I_m \sin(\omega t) \\ u_{\beta o} = \omega L_m I_m \cos(\omega t + \pi/2) + r_m I_m \cos(\omega t) \\ u_{co} = -\sqrt{2}\omega L I_m \sin(\omega t + 3\pi/4) - \sqrt{2} I_m r \sin(\omega t + \pi/4) \end{cases} \quad (10)$$

where, $L_m = L + L_1 = L + L_2$ and $r_m = r + r_1 = r + r_2$. So the total output power of TPOPS is:

$$\begin{aligned} P_o &= u_{\alpha o} i_\alpha + u_{\beta o} i_\beta + u_{co} i_c \\ &= r_m I_m^2 + r I_m^2 + \omega L I_m^2 \cos(2\omega t) + r I_m^2 \sin(2\omega t) \end{aligned} \quad (11)$$

According to the principle of power balance, ignoring the power loss of TPOPS, the dc active power component of P_o should meet the following equation:

$$(r_m + r) I_m^2 = (r_{\delta 1} + r_{\delta 2} + 2r) I_m^2 = 3UI_p / 2 = P_d \quad (12)$$

Therefore, the dc active power absorbed by PWM rectifier is mainly consumed as the work of the electromagnetic force.

2.3 The calculation of 2nd ripple in dc-link voltage

As there is a secondary power P_2 in output power of TPOPS shown as (11), and there is:

$$P_2 = \omega L I_m^2 \cos(2\omega t) + r I_m^2 \sin(2\omega t) \quad (13)$$

According to the principle of power balance, there would be a secondary ripple in dc-link voltage. Assuming the dc-link voltage is $u_{dc} = U_d + \delta\sin(2\omega t + \phi)$, U_d is the dc component, and $\delta\sin(2\omega t + \phi)$ is the voltage ripple. As the instantaneous power of dc-link capacitors is:

$$\begin{aligned} & u_{dc} * C * du_{dc} / dt \\ & = C[U_d + \delta\sin(2\omega t + \phi)] * 2\omega\delta\cos(2\omega t + \phi) \\ & = 2\omega\delta C U_d \cos(2\omega t + \phi) + \omega\delta^2 C \sin(4\omega t + 2\phi) \end{aligned} \quad (14)$$

where, C is the total capacitance of dc-link capacitors. If neglect the 4th ripple, according to the power balance between dc- and ac-link of TPOPS, it can be obtained as:

$$2\omega C U_d \delta\cos(2\omega t + \phi) = \omega L I_m^2 \cos(2\omega t) + r I_m^2 \sin(2\omega t) \quad (15)$$

So the 2nd ripple in dc-link voltage can be derived as:

$$\delta\sin(2\omega t + \phi) = \frac{\omega L I_m^2 \sin(2\omega t) - r I_m^2 \cos(2\omega t)}{2\omega C U_d} \quad (16)$$

According to power analysis above, a 2nd ripple would exist in dc-link voltage, and its frequency is 2-times of output frequency. The amplitude of ripple is proportional to the square of output current, and it is inversely proportional to the capacitance and dc-link voltage.

3. The Integrated Control Method of PWM Rectifier

According to the power analysis above, an integrated control method is proposed for PWM rectifier shown as Fig. 3. It is mainly composed of voltage outer-loop and current inner-loop. According to the analysis in Section.II, there is a 2nd ripple in dc-link voltage. If it is not eliminated in voltage outer-loop, it will generate some additional harmonic instructions for current inner-loop. And then it would produce some harmonic currents in the input of PWM rectifier. The calculation of additional harmonic instruction signals is as follows:

The voltage error Δu is processed by a PI controller, and then its output will be multiplied with the synchronous signal $\sin\omega_o t$ shown as Fig. 3. Assuming the expression of voltage PI controller is $k+k_i/s$, the additional harmonic instruction signal generated by the 2nd voltage ripple is:

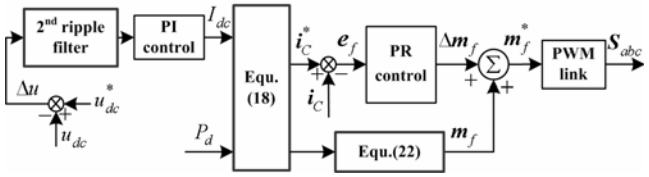

Fig. 3. The integrated control diagram of PWM rectifier

$$\begin{aligned} & [k\Delta u + k_i\int\Delta u] * \sin\omega_o t \\ & = [k\delta\sin(2\omega t + \phi) - \frac{k_i\delta}{2\omega}\cos(2\omega t + \phi)] * \sin\omega_o t \\ & \approx k\delta[\cos((2\omega - \omega_o)t + \phi) - \cos((2\omega + \omega_o)t + \phi)] / 2 \end{aligned} \quad (17)$$

Seen from (17), it would generate two kinds of harmonic instruction signals. The frequencies of harmonic signals are $2\omega \pm \omega_o$, and its amplitude is $k\delta/2$. Therefore, a ripple filter method is proposed for voltage outer-loop, which can eliminate the 2nd ripple and realize the normal control of dc-link voltage. The 2nd ripple expressed as (16) can be adopted to subtract from the voltage error Δu, then the pure dc error can be got for voltage controller shown as Fig. 3. So the output instruction I_{dc} of voltage controller is dc component without ac ripples. However, in the status of alternate rotation process, the system parameters will be varied. As the α- and β-phase equivalent impedances of EM stirrer are generally symmetrical, the ripple elimination method also can be used for voltage control at this time.

According to I_{dc} and active power P_d of EM stirrer, the current instruction signals $i_C^*(i_{Ca}^*, i_{Cb}^*, i_{Cc}^*)$ of PWM rectifier can be obtained as:

$$\begin{cases} i_{Ca}^* = (I_{dc} + \dfrac{2P_d}{3U})\sin\omega_o t \\ i_{Cb}^* = (I_{dc} + \dfrac{2P_d}{3U})\sin(\omega_o t - 2\pi/3) \\ i_{Cc}^* = (I_{dc} + \dfrac{2P_d}{3U})\sin(\omega_o t + 2\pi/3) \end{cases} \quad (18)$$

According to (18), the expected input currents of PWM rectifier can be obtained. As the active currents are ac signals, the traditional PI controller has a limited tracking performance and there would be a control error in the steady-state. Therefore, the proportional resonant (PR) controller was put forward to improve the control performance for ac signals in [21, 22]. The s-domain function of PR controller can be expressed as:

$$G_i(s) = k_p + 2k_i / (s^2 + \omega_o^2) \quad (19)$$

where, k_p is the proportional coefficient, k_i is the integral coefficient. According to the current tracking errors, the control output of current closed-loop can be got by PR controller. So a closed-loop dynamic adjustment of output current can be achieved in the steady state.

According to the circuit shown as Fig. 1, the output voltages of PWM rectifier can be obtained as:

$$\begin{cases} u_{an} = u_{sa} - L_o di_{ca}/dt = u_{sa} - u_{La} \\ u_{bn} = u_{sb} - L_o di_{cb}/dt = u_{sb} - u_{Lb} \\ u_{cn} = u_{sc} - L_o di_{cc}/dt = u_{sb} - u_{Lc} \end{cases} \quad (20)$$

So the modulation signals of PWM rectifier can be obtained as:

$$\begin{cases} m_a = 2u_{an}/u_{dc} = 2(u_{sa} - u_{La})/u_{dc} \\ m_b = 2u_{bn}/u_{dc} = 2(u_{sb} - u_{Lb})/u_{dc} \\ m_c = 2u_{cn}/u_{dc} = 2(u_{sb} - u_{Lc})/u_{dc} \end{cases} \quad (21)$$

The modulation signals are derived from the switching model of PWM converter, and they can be used as the feedforward instruction signals of PWM rectifier. Associate (18) with (21), the expected feedforward instruction signals of PWM rectifier can be obtained as:

$$\begin{cases} m_{fa} = \dfrac{2}{u_{dc}}[U\sin\omega_o t - \omega_o L_o(I_{dc} + \dfrac{2P_d}{3U})\sin(\omega_o t + \dfrac{\pi}{2})] \\ m_{fb} = \dfrac{2}{u_{dc}}[U\sin(\omega_o t - \dfrac{2\pi}{3}) - \omega_o L_o(I_{dc} + \dfrac{2P_d}{3U})\sin(\omega_o t - \dfrac{\pi}{6})] \\ m_{fc} = \dfrac{2}{u_{dc}}[U\sin(\omega_o t + \dfrac{2\pi}{3}) - \omega_o L_o(I_{dc} + \dfrac{2P_d}{3U})\sin(\omega_1 t + \dfrac{7\pi}{6})] \end{cases} \quad (22)$$

So the control system can fast regulate the output of PWM rectifier according to (22), as well as tracking to the change of instruction signals rapidly. By combining the outputs Δm_f of PR controller with the outputs $\boldsymbol{m}_f$ of feedforward control shown as Fig. 3, the total modulation signals $\boldsymbol{m}_f^*$ ($\boldsymbol{m}_{fa}^*$, $\boldsymbol{m}_{fb}^*$, $\boldsymbol{m}_{fc}^*$) of PWM rectifier can be obtained. According to $\boldsymbol{m}_f^*$, the switching signals can be generated by PWM link, and then it can be used to drive power switches and output the desired voltage.

In order to improve the performance of PWM rectifier, a feedforward control method is added in the voltage outer-loop and current inner-loop respectively. According to the system's power analysis, the feedforward signal $2P_d/(3U)$ for voltage outer-loop can be calculated; similarly, in order to improve current inner-loop, a feedforward control signal shown as (22) is used to inhibit the output oscillations of PR controller, and reduce the dynamic adjustment process of current control. Meanwhile, PR controller can be used to improve current control accuracy of PWM rectifier in the steady-state. In this way, the integrated control method can effectively improve the dynamic performance of system, and maintain a stable dc source for the back inverter.

4. The Current Control Method of Two-phase Inverter

As the former PWM rectifier is mainly used to provide a stable dc voltage source, the back TPTLI can be controlled independently. The current composite control diagram of TPTLI is proposed as Fig. 4(a).

Firstly, according to the desired amplitude I_m^* and frequency f^* of output currents which are determined by the continuous casting process of molten steel [25], the desired output currents of TPTLI can be obtained as:

$$\begin{cases} i_\alpha^* = I_m^* \sin\omega^* t \\ i_\beta^* = I_m^* \cos\omega^* t \\ i_c^* = -\sqrt{2} I_m^* \sin(\omega^* t + \pi/4) \end{cases} \quad (23)$$

where, $\omega^* = 2\pi f^*$. Since the load EM stirring is inductive, the amplitude of current instructions is given linearly by the ramp function during the process of positive and negative alternate rotation. The desired output currents i_α^*, i_β^*, i_c^* subtract the output currents of inverter respectively, then the current errors can be obtained. And then the dynamic modulation signals $\Delta u_{t\alpha}$, $\Delta u_{t\beta}$, Δu_{tc} of TPTLI can be obtained by PR controller shown as Fig. 4(a). These modulation signals are mainly used to carry out the closed-loop tracking control according to current errors.

According to simplified equivalent model of EM stirrer and (10), the feedforward modulation signals of TPTLI for each switch leg can be gained as:

$$\begin{cases} u_{t\alpha} = 2[\omega L_m I_m^* \sin(\omega^* t + \pi/2) + r_m I_m^* \sin(\omega^* t)]/u_{dc} \\ u_{t\beta} = 2[\omega L_m I_m^* \cos(\omega^* t + \pi/2) + r_m I_m^* \cos(\omega^* t)]/u_{dc} \\ u_{tc} = -2[\sqrt{2}\omega L I_m^* \sin(\omega^* t + 3\pi/4) \\ \qquad + \sqrt{2} I_m^* r \sin(\omega^* t + \pi/4)]/u_{dc} \end{cases} \quad (24)$$

If the current instructions change, these feedforward modulation signals would change correspondingly. So it can rapidly regulate the output voltages of inverter according to the instruction currents. Similarly with the current control of PWM rectifier, this current composite control method can combine the merits of feedforward control and feedback control. So it can effectively improve the tracking performance of inverter to meet the requirements of fast alternate rotation of EM stirring.

In order to further analyze the tracking characteristic of current composite control method for inverter, the closed-loop control diagram is established shown as Fig. 4(b). In Fig. 4(b), k_g is the normalized parameter, equal to $2/u_{dc}$; e^{-Ts} is the output delay link, which means that the output delays a control cycle T, and it can be simplified as $(1-0.5Ts)/(1+0.5Ts)$ by 1st order pade approximation [23]; $H(s)$ is the detection feedback link, which can be considered as $1/(\tau s+1)$; k_{PWM} is the gain of PWM link, and it is equal to $u_{dc}/2$; $Z_d(s)$ is the equivalent impedance of load, and it is equal to $L_m s + r_m$.

Seen from Fig. 4(b), assuming:

$$G_1(s) = \frac{k_g * k_{PWM} * e^{-Ts}}{Z_d(s)} = \frac{(1-0.5Ts)}{(1+0.5Ts)Z_d(s)} \quad (25)$$

Then the open-loop transfer function of inverter can be expressed as:

$$G_o(s) = [G_i(s) + Z_d(s)]G_1(s) \tag{26}$$

The error-tracking transfer function of inverter can be expressed as:

$$G_e(s) = \frac{e_i}{i_r} = \frac{1 - Z_d(s)G_1(s)H(s)}{1 + G_i(s)G_1(s)H(s)} \tag{27}$$

In Fig. 4(c), it can be seen that when using the composite control method, the gain of open-loop control characteristic is basically 1 at the high-frequency range. It means that the composite control method can realize a quick response to high-frequency input signal and improve the dynamic performance of inverter. At the same time, when only using the traditional feedback control method, the gain of open-loop control of system is attenuated at the high-frequency range. So the dynamic response of system with the proposed control method will be better than the one with the traditional control method.

Seen from Fig. 4(d), when using the composite control method, the error-tracking characteristic of system at the low-frequency working range is attenuated more seriously than traditional control method. The control error at the low-frequency working range with proposed control method would be smaller, so the control precision can be improved.

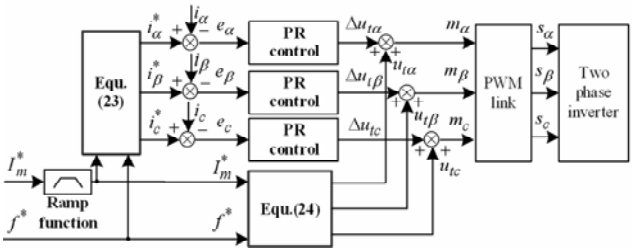

(a) the current composite control diagram of TPTLI

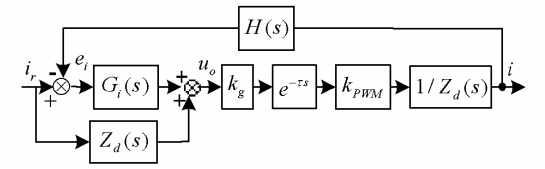

(b) the control block diagram of TPTLI in s domain

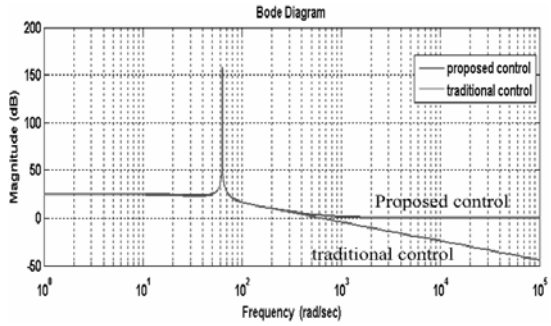

(c) the comparison of open-loop control performance

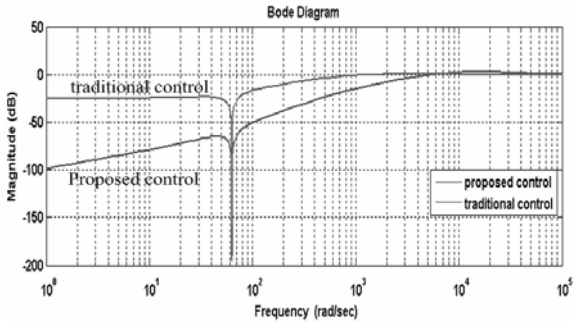

(d) the comparison of error-tracking performance

Fig. 4. The control diagram of TPTLI and the performance comparison

5. Simulation and Experimental Results

5.1 Simulation results

To verify the analysis and control method of TPOPS proposed in the paper, the simulation of TPOPS shown as Fig. 1 is built by using software PSIM.9. The three-phase source is 380V/50Hz. This design of TPOPS is used for a production line of 200*200mm billet continuous casting. According to the theory and practice of EM stirring [25], the rated output current is set as 400A and the rated output frequency is set as 10Hz. In the steady-state, the output capacity of TPOPS is 300kVA, and the rated output active power and reactive power are 90kW, 286kVar, respectively. The design of main circuit and control parameters of TPOPS are presented in the appendix. The parameter values of system are shown as Table 1.

Before put into the EM stirring load, the dc-link voltage is stable at 750V by PWM rectification. At 0.4s, the EM stirring load is put into system. In Fig. 5, I1, I2, I3 are the output currents of TPOPS respectively. Since the EM stirring load is inductive, the amplitude of output current instructions is given linearly. From 0.4s to 0.6s, the amplitude of current instructions is increased from 0 to

Table 1. Parameters of TPOPS

System parameter	Value
circuit parameter	
input inductor	L_o=1mH; r_o=0.02 Ω
dc-link capacitor	C=10000uF
output inductor	L=0.5mH; r=0.01 Ω
PWM rectifier	Capacity: 120kVA
Two-phase inverter	Capacity: 300kVA
dc-link voltage	750V
rated output current	400A
rated output frequency	10Hz
control frequency	10kHz
control parameter	
Voltage PI controller of PWM rectifier	2(1+10/s)
Current PR controller of PWM rectifier	10+2*120s/(s^2+ ω_o^2)
Current PR controller of inverter	5+2*80s/(s^2+ ω^2)

566A. Seen from Fig. 5(a), the output currents of inverter increase linearly from 0 at 0.4s, and almost reach a stable state at 0.6s. Meanwhile, the active power of load almost increases as the square of output currents. With the proposed control method, PWM rectifier can fast track to the change of output active power. Shown as Fig. 5(b), the input currents of PWM rectifier approximate to increase quadratically, and it almost gets into the steady state at 0.6s. The change of input currents is nearly synchronous with the variation of output currents, so the proposed control method can effectively improve the tracking performance of PWM rectifier to maintain dc-link voltage stably shown as Fig. 5(c). According to the analysis in Section. II, there is a 2nd ripple in dc-link voltage shown as Fig. 5(c), and the amplitude of ripple is almost increasing with the rise of output currents.

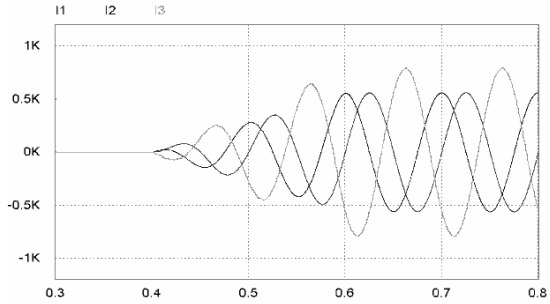

(a) the output current dynamic waveform of TPOPS

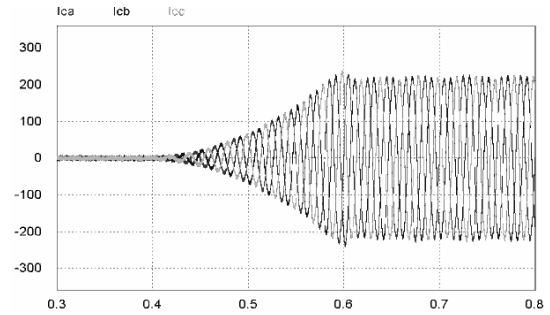

(b) the input current dynamic waveform of TPOPS

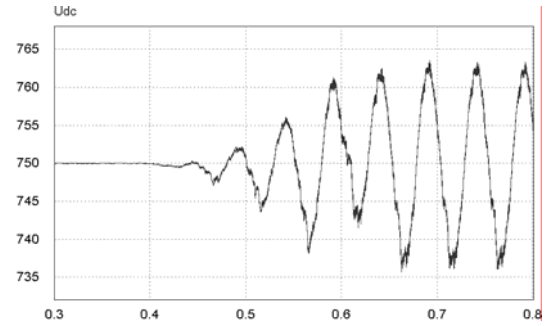

(c) the dynamic waveform of dc-link voltage

Fig. 5. The dynamical waveforms when switching into the EM stirring load

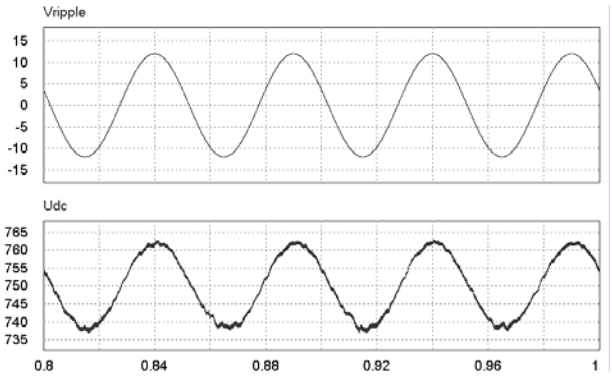

(a) the contrastive waveforms of the 2nd ripple

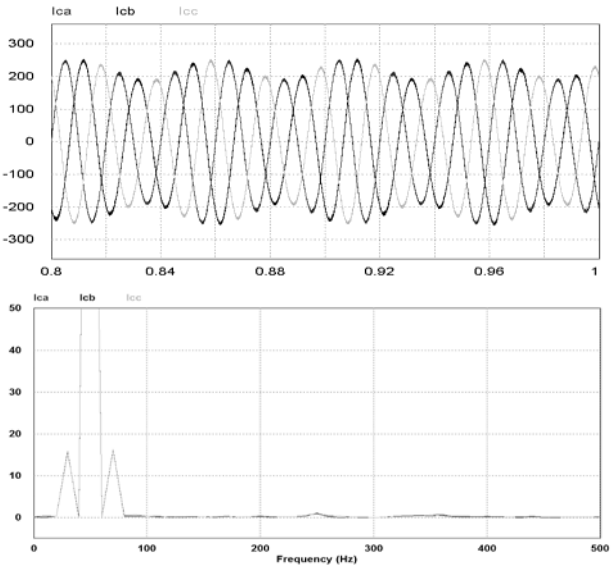

(b) the input current waveforms and their spectrums without the ripple filter

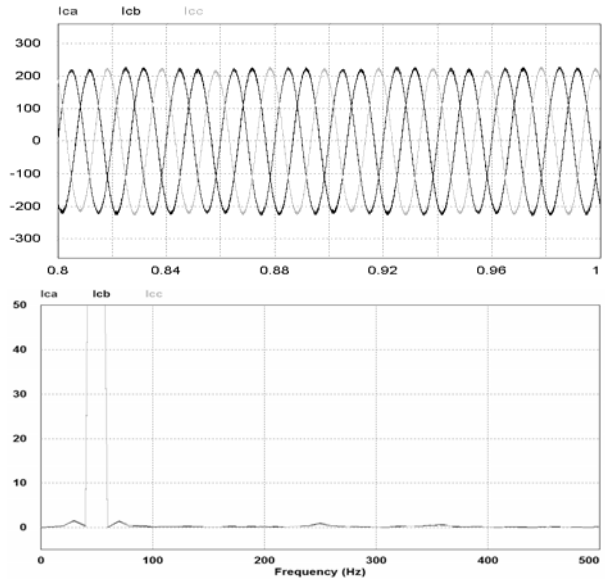

(c) the input current waveforms and their spectrums with the ripple filter

Fig. 6. The contrast waveforms for the ripple filter

In order to verify the ripple filter method, a simulation comparison is carried out. In Fig. 6(a), 'Udc' is the detected dc-link voltage; 'Vripple' is the value calculated by (16). In the steady-state the detected ripple in dc-link voltage is almost the same as the calculated ripple. In Fig. 6(a), the amplitude of the ripple is about 14V and its frequency is 20Hz.

Fig. 6(b) represents the current waveforms and spectrums without using the ripple filter method respectively. As the dc-link voltage contains a 2nd ripple, after the adjustment of PI controller, the ripple would be multiplied with the synchronous signal. Then it would generate two kinds of additional harmonic instruction signals for current inner-loop, of which the frequencies are 30Hz and 70Hz respectively shown as (17). By the closed-loop control of current controller, the input currents of PWM rectifier would contain these two kinds of harmonic currents shown as Fig. 6(b). The amplitude of these two harmonics are both about 15A shown as the spectrums in Fig. 6(b), so it is basically consistent with the analysis in Section.III. Fig. 6(c) represents the current waveforms and spectrums with using the ripple filter method. The ripple can be calculated as (16), then it can be eliminated from the voltage error and the pure dc error can be obtained for voltage PI controller. So the voltage controller would not produce additional harmonic instructions for current controller, and there is little harmonic current in input currents shown as the spectrums in Fig. 6(c). Therefore, the voltage controller of PWM rectifier can operate normally without adding a lower pass filter to attenuate the ac ripples.

As shown in Fig. 6(c), the amplitude of input currents in the steady-state is 153A. The PF of PWM rectifier is 0.99, and the total harmonic distortion (THD) of current is 3.1%. Therefore, PWM rectifier can effectively improve power quality of TPOPS.

In order to verify the current control method of inverter, the EM stirrer would reversely rotate at 2.0s. The amplitude of α- and β-phase current instructions of TPTLI changes linearly at 1.6s from +566A to 0 within 0.2s, then the inverter would stop working for 0.2s. Finally, the amplitude of α-phase current instruction would increase linearly at 2.0s from 0 to +566A within 0.2s, while the amplitude of β-phase current instruction would increase linearly at 2.0s from 0 to -566A within 0.2s shown as Fig. 7(a). So the reverse rotation of EM stirrer can be achieved.

In Fig. 7(b) and (c), I1, I2, I3 are the output currents of TPTLI respectively, and ie2 represents the tracking error of α-phase output current of inverter. Fig. 7(b) shows the waveforms when only using PR current controller. Since the output current instructions of inverter are changing, the modulation signals of inverter are completely from the output of PR controller. The PR controller is a current feedback control, which has a relatively lag to response, so there is a piece of vibration process in the tracking error. The maximum peak of tracking error is almost 20A shown as Fig. 7(b). When using the proposed current control

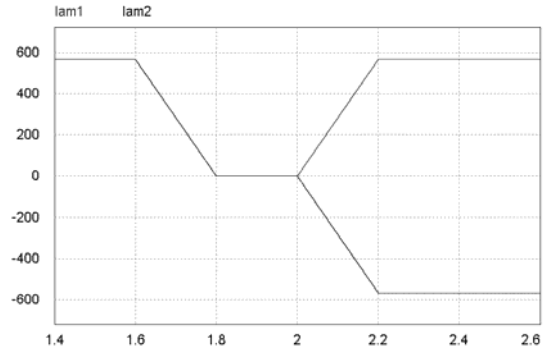

(a) the given amplitude of α- and β-phase currents

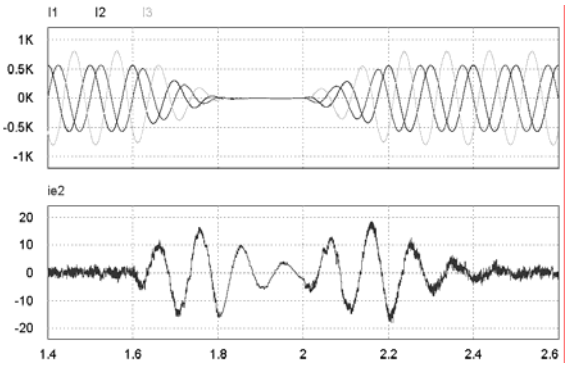

(b) the output currents only with PR control method

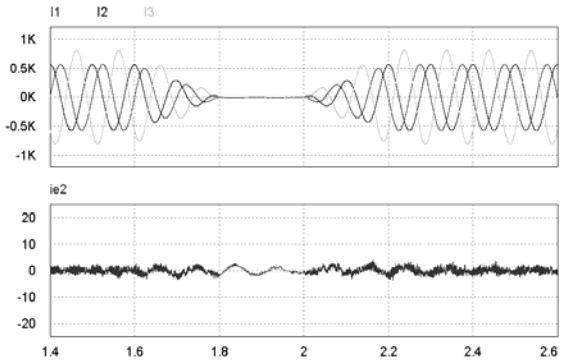

(c) the output currents with the proposed composite control method

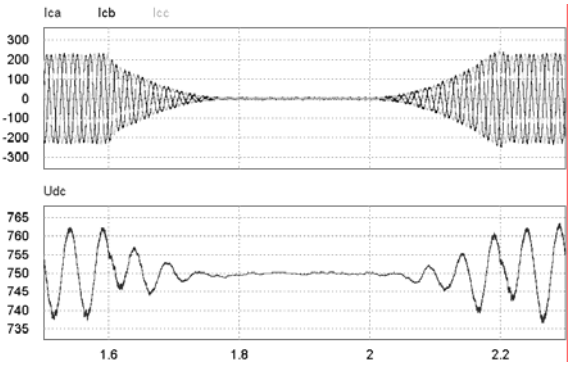

(d) the input currents of PWM rectifier and dc-link voltage

Fig. 7. The current and voltage waveforms during the period of alternate rotation

method, the dynamical waveforms are shown as Fig. 7(c). Since the feedforward signals shown as (24) are obtained from the model of EM stirrer, it can fast control TPTLI to output the corresponding voltages according to the instruction currents. When the current instructions change, the feedforward signals would be varied at the same time. So the current tracking error is almost without vibrations shown as Fig. 7(c). Meanwhile, by using PR feedback control, it can achieve a closed-loop tracking to the current instruction signals and improve the control precision. Therefore, the proposed composite control method can effectively improve the tracking performance of inverter, so as to meet the requirements of fast alternate rotation of EM stirrer.

Fig. 7(d) shows the input currents and dc-link voltage of PWM rectifier with the proposed control method during the period of alternate rotation. The input currents of PWM rectifier almost follow the change of output currents, therefore, PWM rectifier can fast track the change of load power. And with the change of output currents, the 2nd ripple of dc-link voltage is varied correspondingly.

5.2 Experimental results

In order to further verify the analysis and control method, a 300kVA-380V low-frequency TPOPS for EM stirrer is developed, and the physical layout diagram of TPOPS is shown as Fig. 8(a). PWM rectifier and three-leg inverter adopt a TMS320F2812 separately as the digital signal processor (DSP), which is used to sample signals, execute algorithm and generate PWM drive signals for IGBTs. The A-phase voltage is processed by zero-crossing comparison circuit, which is used to generate an interrupt for DSP to initialize the phase angle. The temperature of cooling water in EM stirrer is sampled for protection and two DSPs are communicated with each other by RS232. The system parameters of device for experiments are shown in Table. 1. The control frequency of power switches is 10kHz. Fig. 8(b) and (c) are the physical photos of TPOPS, while Fig. 9 and Fig. 10 are the experimental waveforms.

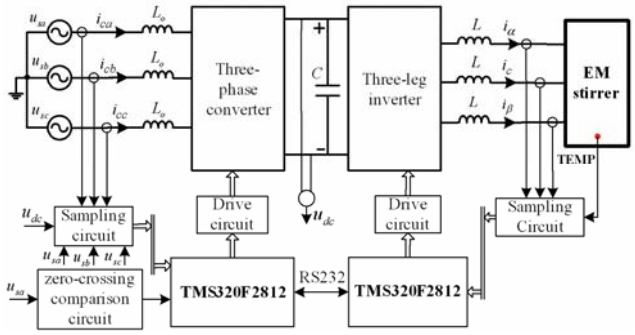

(a) the physical layout diagram of TPOPS

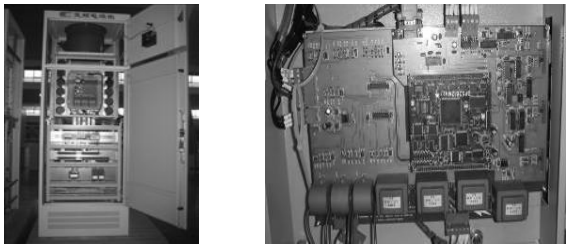

(b) the photo of TPOPS (c) the photo of DSP control panel

Fig. 8. The physical implementation pictures of TPOPS

Seen from Fig. 9, it shows the dynamic waveforms when the EM stirrer is in the status of positive and negative alternate rotation. With the proposed control method for TPOPS, the output currents of inverter can change rapidly,

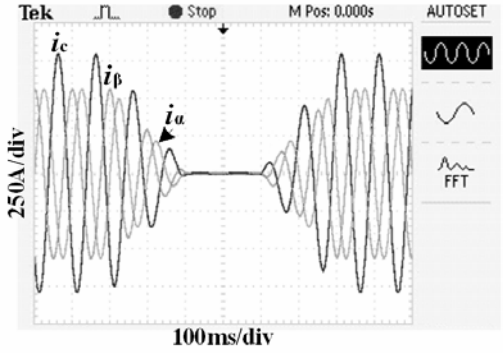

(a) the output currents of TPOPS

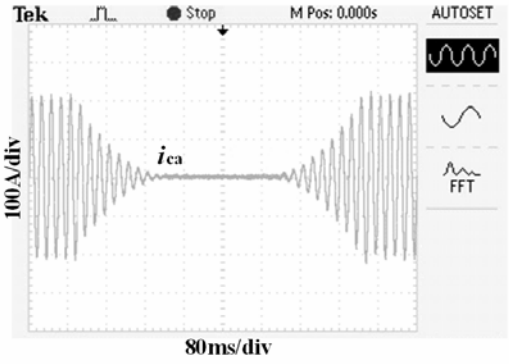

(b) the a-phase input current of PWM rectifier

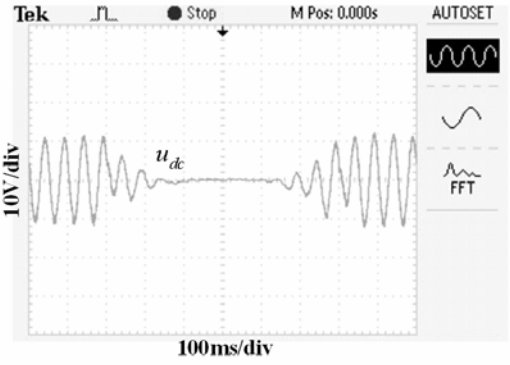

(c) the dc-link voltage

Fig. 9. Experimental waveforms during the period of alternate rotation

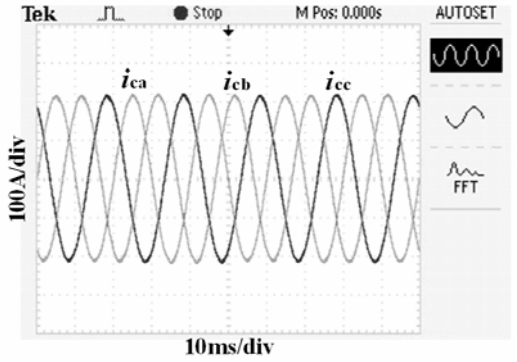

(a) the input currents of PWM rectifier

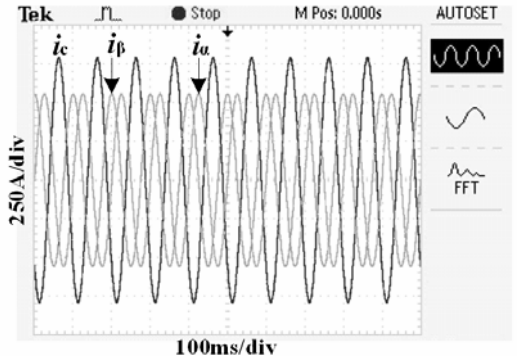

(b) the output currents of TPOPS

Fig. 10. Experimental waveforms in the steady-state

and the a-phase input current of PWM rectifier can follow the change correspondingly shown as Fig. 9(b). Seen from Fig. 9(c), there is a 20Hz ripple in dc-link voltage and it is varied with the change of output currents. When the output currents are 0, the ripple is almost 0 and the dc-link voltage is stable at 750V. Fig. 10 is experimental waveforms in the steady-state. The input currents of PWM rectifier are about 155A. The PF of PWM rectifier is 0.98, and the THD of current is 4.3% shown as Fig. 10(a). While the output currents of TPOPS are about 401A, and the THD of current is 3.4% shown as Fig. 10(b).

The TPOPS with the proposed control method has been installed successfully on production line of the billet continuous casting. With the proposed control method, the period of alternate rotation of EM stirring is reduced. So it can enhance the effective work time of EM stirring and it can make the stirring of molten steel more symmetrically and uniformly. The equiaxed crystal rate of special steel billet is increased from 30% to 53%. Finally, the rate of finished products increases by 5%.

6. Conclusion

In order to improve the quality of billet continuous casting, a kind of TPOPS is researched which is composed of PWM rectifier and three-leg inverter. According to the circuit structure of TPOPS, the power model of system is analyzed. According to the power analysis, an integrated control method with feed-forward control for PWM rectifier is proposed, while a current composite control method is proposed for inverter to improve the output tracking performance. The closed-loop control diagram in *s*-domain is established, and the design of control parameters is presented. With the work of proposed control system, the dynamic performance of TPOPS is effectively improved which can meet the requirements of fast and frequent alternate rotation of EM stirring.

Acknowledgements

The financial support of Hunan Provincial Innovation Foundation For Postgraduate (Project No. CX2012A006) and The National Basic Research Program of China (973 Program) (Project No. 2009CB219706) are highly acknowledged.

Appendix

A. The main circuit parameter design of TPOPS

In order to meet the requirements of fast tracking performance and current ripple inhibition, a proper filter inductance is expected. According to [24] and [11], on the basis of the maximum allowable current ripples ($\Delta I_{1\max}$ and $\Delta I_{2\max}$) of PWM rectifier and inverter respectively, L_o and L can be designed as:

$$\frac{(2U_d - 3U)U^* T}{2U_d \Delta I_{1\max}} \le L_o \le \frac{2U_d}{3\omega_o I_p} \tag{28}$$

$$\frac{U_d T}{2\Delta I_{2\max}} - L_1 \le L \le \frac{U_d}{\omega I_m} - L_1 \tag{29}$$

Where, T is the PWM control period; I_p and I_m are the current amplitude of PWM rectifier and inverter respectively. According to (16), the voltage ripple of dc-link capacitors is $\delta \sin(2\omega t + \phi)$. Then the maximum amplitude of voltage ripple is:

$$\max\left|\frac{\omega L I_m^2 \sin(2\omega t) - r I_m^2 \cos(2\omega t)}{2\omega C U_d}\right| \approx \frac{\omega L I_m^2}{2\omega C U_d} \tag{30}$$

Assuming $\Delta\varsigma_{\max}$ is the limit value of voltage ripple, there is:

$$C > \omega L I_m^2 / (2\omega \Delta\varsigma_{\max} U_d) \tag{31}$$

B. The control parameter design of TPOPS

According to the design method of controllers in [24],

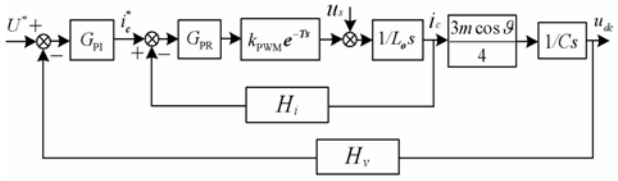

Fig. 11. The control block diagram for PWM link in *s*-domain

the voltage and current dual-loop control diagram of PWM rectifier in s-domain can be established shown as Fig. 11. In Fig. 11, H_i and H_v are the voltage and current sampling functions respectively, which can be simplified as $1/(\tau s+1)$. k_{pwm} is the gain of PWM link; e^{-Ts} is the output delay link, and it can be simplified as $(1-0.5Ts)/(1+0.5Ts)$.

According to Fig. 11, the open-loop transfer function of current inner-loop can be obtained as:

$$G_{io}=\frac{G_{\mathrm{PR}}*k_{\mathrm{PWM}}*H_i*(1-0.5Ts)}{L_o s*(1+0.5Ts)} \tag{32}$$

According to bode diagram analysis of open-loop system, considering the system stability and response speed, a set of proper control parameters are selected as: $k_{p1}=10$, $k_{i1}=120$.

Since the response bandwidth of current inner-loop is much wider than the one of voltage outer-loop, so the transfer function of current inner-loop can be seen as 1 when designing voltage outer-loop. In Fig. 11, $0.75m\cos\vartheta$ is the equivalent transfer function from ac current i to dc current i_{dc} [24], and it is simplified as 0.75. Therefore, the open loop transfer function of voltage outer-loop can be obtained as:

$$G_{vo}=0.75G_{\mathrm{PI}}*H_v/Cs \tag{33}$$

According to bode diagram analysis of open-loop system, the control parameter of PI controller can be designed as: $G_{\mathrm{PI}}=2(1+10/s)$.

As the control diagram of inverter in *s*-domain is established shown as Fig. 4(b), and the open-loop transfer function of system is expressed as (26). According to bode diagram analysis of open-loop system, a set of proper control parameters for current PR controller are selected as: $k_{p2}=5$, $k_{i2}=80$.

References

[1] Trindade, L.B.; Vilela, A.C.F.; Filho, A.F.F.; et al,"Numerical model of electromagnetic stirring for continuous casting billets", *IEEE Trans. Magnetics*, vol. 38, no. 6, pp. 3658-3660, 2002

[2] Osman Kalfinaler and Yavuz Ege, "A PIC Micro-controller Based Electromagnetic Stirrer", *IEEE trans. magnetics*, vol. 43, no. 9, pp. 3579-3584, 2007.

[3] Cheng-Tsung Liu, "In-Mold Electromagnetic Stirrer", *IEEE Industry Applications Magazine*, vol. 16, no. 2, pp. 56-61, 2010

[4] Cheng-tsung liu, Sheng-yang lin, Weng-jay lee, Jen-hsin chen, "Electromagnetic Stirring Systems", *IEEE industry applications magazine*, vol. 17, no. 2, pp. 38-43, 2011.

[5] Otake, R.; Yamada, T.; Hirayama, R.; et al, "Effects of Double-Axis Electromagnetic Stirring in Continuous Casting", *IEEE Trans. Magnetics*, vol. 44, no. 11, pp. 4517-4520, 2008

[6] Ege, Y.; Kalender, O.; Nazlibilek, S, "Electromagnetic Stirrer Operating in Double Axis", *IEEE Trans. Industrial Electronics*, vol. 57, no. 7, pp. 2444-2453, 2010

[7] Rojat, G.; Mertz, J.L.; Foggia, A, "Theoretical and Experimental Analysis of a Two-Phase Inverter-Fed Induction Motor", *IEEE Trans. Industry Applications*, Vol. IA-15, no. 6, pp. 601-605, 1979

[8] Shin-ichi Furuya, Tom Maruhashi, Yuji Izuno, and Mutsuo Nakaoka, "Load-Adaptive Frequency Tracking Control Implementation of Two-Phase Resonant Inverter for Ultrasonic Motor", *IEEE trans. power electronics*, vol. 7, no. 3, pp. 542-550, 1992.

[9] Young, C.-M.; Liu, C.-C.; Liu, C.-H, "New inverter-driven design and control method for two-phase induction motor drives", *IEE Proceedings-Electric Power Applications*, Vol. 143, no. 6, pp. 458-466, 1996

[10] Do-Hyun Jang, Duck-Yong Yoon, "Space-Vector PWM Technique for Two-Phase Inverter-Fed Two-Phase Induction Motors", *IEEE Trans. on industry applications*, vol. 39, no. 2, pp. 542-549, 2003.

[11] An Luo, Huagen Xiao, Honglin Ouyang, Chuanping Wu, et al, "Development and Application of the Two-Phase Orthogonal Power Supply for Electromagnetic Stirring", *IEEE Trans. power electronics*, vol. 28, no. 7, pp. 3438-3446, 2013.

[12] M. A. Jabbar, Ashwin M. Khambadkone, and Zhang Yanfeng, "Space-Vector Modulation in a Two-Phase Induction Motor Drive for Constant-Power Operation", *IEEE trans. industrial electronics*, vol. 51, no. 5, pp. 1081-1088, 2004.

[13] DO-HYUN JANG, "PWM methods for two-phase inverters", *IEEE industry applications magazine*, vol. 13, no. 2, pp. 50-61, 2007.

[14] Tomaselli, L.C.; Lazzarin, T.B.; Martins, D.C.; Barbi, I, "Application of the Vector Modulation in the Symmetrical Two-Phase Induction Machine Drive", *IEEE 36th Power Electronics Specialists Conference*, 2005, pp. 1253-1258

[15] Taufik; Tam, Y.; Anwari, M, "Comparative study of sinusoidal pulse width and hysteresis modulations in current source inverter", *International Conference on*

Intelligent and Advanced Systems, 2007, pp. 906-911
[16] Sheng-Ming Yang; Feng-Chieh Lin; Ming-Tsung Chen, "Micro-stepping control of a two-phase linear stepping motor with three-phase VSI inverter for high-speed applications", *IEEE Trans. Industry Applications*, Vol. 40, no. 5, pp. 1257-1264, 2004
[17] Maurício Beltrão de Rossiter Corrêa, Cursino Brandão Jacobina,et al, "A Three-Leg Voltage Source Inverter for Two-Phase AC Motor Drive Systems", *IEEE trans. power electronics*, vol. 17, no. 4, pp. 517-523, 2002.
[18] Vijit Kinnares, and Chakrapong Charumit, "Modulating Functions of Space Vector PWM for Three-Leg VSI-Fed Unbalanced Two-Phase Induction Motors", *IEEE Trans. power electronics*, vol. 24, no. 4, pp. 1135-1139, 2009.
[19] YUAN Chao, "The Research of electromagnetic stirring technique System", Master's Thesis, Hunan University, China, 2011.
[20] Peng Hongcai, "Principle of electric machine and drag:1st edn", China Machine Press, 2006, pp.135-178. [in Chinese]
[21] Zhong, Q.C; Hornik, T, "Current Proportional-Resonant Control", *Control of Power Inverters in Renewable Energy and Smart Grid Integration*, 2012, pp. 259-268
[22] Holmes, D.G.; Lipo, T.A.; McGrath, B.P.; Kong, W.Y., "Optimized Design of Stationary Frame Three Phase AC Current Regulators", *IEEE Trans. Power Electronics*, Vol. 24, no. 11, pp. 2417-2426, 2009
[23] Wang Xuelei, Shao Huihe, "New method of frequency domain identification and model reduction based on Pade approximation", *Control theory & Applications*, vol. 20, no. 1, pp. 54-58, 2003.
[24] Xing, Z., Chongwei, Z. "PWM rectifier and its control: 1st edn", China Machine Press, 2012, pp. 88-98
[25] Mao, B., Guifang Zhang, Aiwu Li. "Theory and Technology of Electromagnetic Stirring for Continuous Casting: 1st edn", Metallurgical Industry Press, 2012, pp. 331-368

Fujun Ma received B.S. degree from college of electrical and information engineering, Hunan University, Changsha, China, in 2008. He is pursuing his Ph.D. degree from college of electrical and information engineering, Hunan University. He is currently an Associate Professor in Hunan University, Changsha, China. His research interests are power quality management, active power filtering and industrial power converter and power electronic system.

An Luo received the B.S. and M.S. degrees from Hunan University, Changsha, in 1982 and 1986, respectively, and the Ph.D. degree from Zhe-jiang University, Zhejiang, China, in 1993.
Between 1996 and 2002, he was a Professor with the Central South University. In 2003, he became a Professor at Hunan University, where he is currently involved in research on power conversion system, harmonics suppression and reactive power compensation, and electric power saving. He has published more than 300 journal and conference articles. He also serves as the Chief of Hunan Electric Science and Application Laboratory.
Dr. Luo is a recipient of the 2006 National Scientific and Technological Awards of China, and the 2010 National Scientific and Technological Awards of China. He currently serves as the Associate Board Chairperson of the Hunan Society for Electrical Engineering.

Qiaopo Xiong received B.S. degree from school of information science and engineering, Central South University, Changsha, China, in 2009. He received Ph.D. degree from college of electrical and information engineering, Hunan University, Changsha, China, in 2014. He is currently an Associate Research Engineer in 722th Research Institute of CSIC, Wuhan, Hubei Province, China. His research interests are VSC high-voltage direct current system, static var compensator and modular multilevel system design.